© 2015. Published by The Company of Biologists Ltd | Development (2015) 142, 465-476 doi:10.1242/dev.112946

RESEARCH ARTICLE

STEM CELLS AND REGENERATION

Mediator *Med23* deficiency enhances neural differentiation of murine embryonic stem cells through modulating BMP signaling

Wanqu Zhu, Xiao Yao*, Yan Liang*, Dan Liang, Lu Song, Naihe Jing, Jinsong Li and Gang Wang‡

ABSTRACT

Unraveling the mechanisms underlying early neural differentiation of embryonic stem cells (ESCs) is crucial to developing cell-based therapies of neurodegenerative diseases. Neural fate acquisition is proposed to be controlled by a 'default' mechanism, for which the molecular regulation is not well understood. In this study, we investigated the functional roles of Mediator *Med23* in pluripotency and lineage commitment of murine ESCs. Unexpectedly, we found that, despite the largely unchanged pluripotency and self-renewal of ESCs, *Med23* depletion rendered the cells prone to neural differentiation in different differentiation assays. Knockdown of two other Mediator subunits, *Med1* and *Med15*, did not alter the neural differentiation of ESCs. *Med15* knockdown selectively inhibited endoderm differentiation, suggesting the specificity of cell fate control by distinctive Mediator subunits. Gene profiling revealed that *Med23* depletion attenuated BMP signaling in ESCs. Mechanistically, MED23 modulated *Bmp4* expression by controlling the activity of ETS1, which is involved in *Bmp4* promoter-enhancer communication. Interestingly, *med23* knockdown in zebrafish embryos also enhanced neural development at early embryogenesis, which could be reversed by co-injection of *bmp4* mRNA. Taken together, our study reveals an intrinsic, restrictive role of MED23 in early neural development, thus providing new molecular insights for neural fate determination.

KEY WORDS: BMP signaling, ETS1, MED23, Mediator, Embryonic stem cells, Neural differentiation

INTRODUCTION

Embryonic stem cells (ESCs) are derived from the inner cell mass of growing blastocysts and have been widely used in developmental biology, drug discovery and cell therapies (Crook and Kobayashi, 2008; Kirouac and Zandstra, 2008). Neural induction from ESCs is regulated by many transcription factors and signaling pathways. Two distinct molecular models have been proposed to describe this process. The default model states that neural induction is achieved in absence of inhibitory instruction from bone morphogenetic protein (BMP) signals (Muñoz-Sanjuán and Brivanlou, 2002). Recent studies suggest that fibroblast growth factor (FGF) signaling, collaborating with BMP inhibition, contributes to neural specification (Kunath et al., 2007; Stavridis et al., 2007). Despite multiple signals of neural induction having been identified, it remains unclear how they are internally controlled or interpreted by the cell. A detailed description of molecular and cellular events controlling the generation of neural cell types from ESCs is fundamental to our understanding of neural specification processes and for developing treatments for neurological diseases.

The Mediator complex is an evolutionarily conserved multi-protein complex, connecting transcriptional factors to the mRNA polymerase II apparatus, and contributes to regulating gene activities and biological processes (Kagey et al., 2010; Malik and Roeder, 2010). The Mediator subunit *med23* (*sur2*) was first identified as a genetic modulator for an abnormal viral phenotype in *Caenorhabditis elegans* that resulted from hyperactive Ras signaling (Singh and Han, 1995). Previously, we demonstrated that MED23 physically interacts with the ternary complex factor ELK1 to transduce insulin-MAPK signaling (Wang et al., 2005, 2009). In the mesoderm development, MED23 has been recently shown to function as a 'two-way' switch between Ras/Elk1 and RhoA/Mal signaling, which leads to cell fate preference between the SMC and adipocyte (Yin et al., 2012). Mice lacking MED23 function showed embryonic lethality at around embryonic day (E) 10.5 and the homozygous mutant embryos were smaller than their wild-type littermates (Balamotis et al., 2009). Besides the apparent anomalies in blood vessel formation, E9.5 *Med23*$^{-/-}$ embryos exhibited severely disorganized nervous system and aberrant neural tube closure, indicating that MED23 might play a crucial role in neural development. However, due to the complexity of the *in vivo* environment, the specific function and mechanism of MED23 in early neural development remains to be elucidated.

In this study, we used murine *Med23*$^{-/-}$ (KO) ESCs (mESCs) as an *in vitro* model to investigate the molecular functions of MED23 in pluripotency and cell lineage commitment. We found that *Med23* depletion did not change the pluripotency or self-renewal of ESCs, but significantly promoted neural lineage specification through attenuating BMP signaling. We further demonstrated that MED23 functionally interacts with ETS1 to control BMP4 expression through both its promoter and enhancer functions. Interestingly, morpholino-mediated *med23* knockdown in zebrafish enhanced the neural development at a specific time window of the early development, which was reversible by co-injection of *bmp4* mRNA. These results suggest that MED23 functions as a cell-intrinsic regulator of the early neural development through controlling the ETS1-driven *Bmp4* transcription. Our findings provide mechanistic insights into the transcriptional control of the most crucial factor of the neural 'default' model. This should help in understanding the intricate molecular regulation of neural fate and in developing cell-based therapies of neurodegenerative diseases.

RESULTS

Med23 depletion does not change the stem cell pluripotency

The generation of *Med23* KO ESCs has been described in detail previously (Stevens et al., 2002), and is represented by a schematic diagram here (supplementary material Fig. S1A). To investigate the role of Mediator MED23 in early embryonic development, we

State Key Laboratory of Cell Biology, Institute of Biochemistry and Cell Biology, Shanghai Institutes for Biological Sciences, Chinese Academy of Sciences, Shanghai 200031, China.
*These authors contributed equally to this work

‡Author for correspondence (gwang@sibcb.ac.cn)

Received 20 May 2014; Accepted 30 November 2014

Development (2015) 142, 465-476 doi:10.1242/dev.112946

first examined the self-renewal capability and pluripotency of *Med23* KO ESCs *in vitro*. We initially observed that the KO ESCs formed colonies on MEF feeder cells, similar to wild-type ESCs, and all wild-type and KO ESC colonies were positive for alkaline phosphatase staining (Fig. 1A). Pluripotency marker gene expression, represented by *Oct4* and *Nanog*, was comparable between wild-type and KO ESCs when analyzed by quantitative real-time PCR (qRT-PCR) (Fig. 1B). Global gene expression profiling showed that KO ESCs are similar to wild-type ESCs, with an r^2 value (square of linear correlation coefficient) between KO ESCs and wild-type ESCs of 0.99 (Fig. 1C). Embryoid body (EB) formation is a feature observed in ESCs. KO ESCs were able to grow into EBs similar to those of wild-type ESCs, suggesting that KO ESCs retain many features of ESCs (Fig. 1D). Accordingly, immunostaining revealed no obvious differences in the expression of the pluripotency marker proteins OCT4 and SSEA1 between wild-type and KO ESCs (Fig. 1E). Teratomas generated from either wild-type or KO ESCs implanted subcutaneously in nude mice also successfully differentiated into the three germ layers (Fig. 1F). Unbiased spontaneous differentiation of EBs derived from both wild-type and KO ESCs gave rise to the cell types of all three germ layers, as indicated by real-time PCR analysis of the marker gene expression (Fig. 2A). These results indicate that KO ESCs could differentiate into cells of the three primary germ layers, both *in vivo* and *in vitro*, similar to wild-type ESCs. Finally, considering that *Med23* KO embryos were able to develop to E10.5 and form most tissues and organs (Balamotis et al., 2009), we conclude that the embryonic stem cell features of the *Med23* KO ESCs are largely unchanged by loss of *Med23*.

Med23 deficiency promotes neural lineage specification during spontaneous differentiation

Despite the fact that *Med23* deficiency does not significantly alter the self-renewal ability of ESCs, the full term development of *Med23* KO mice was compromised, suggesting a possible defect in cellular differentiation. Indeed, neural cells appeared to be more abundant in *Med23* KO teratomas than in wild type, and neural cells appeared to be more abundant in *Med23* KO ESC-derived teratomas than in wild-type ESC-derived teratomas (data not shown). This observation prompted us to investigate the function of MED23 in ESC differentiation. Wild-type and KO ESCs were cultured under conditions that favored EB formation without leukemia inhibitory facto (LIF). We observed many rosette structures in KO cells at day 9, whereas rosettes rarely appeared in wild-type cells (supplementary material Fig. S1B,C). The expression of marker genes for all three germ layers was monitored over time by RT-PCR

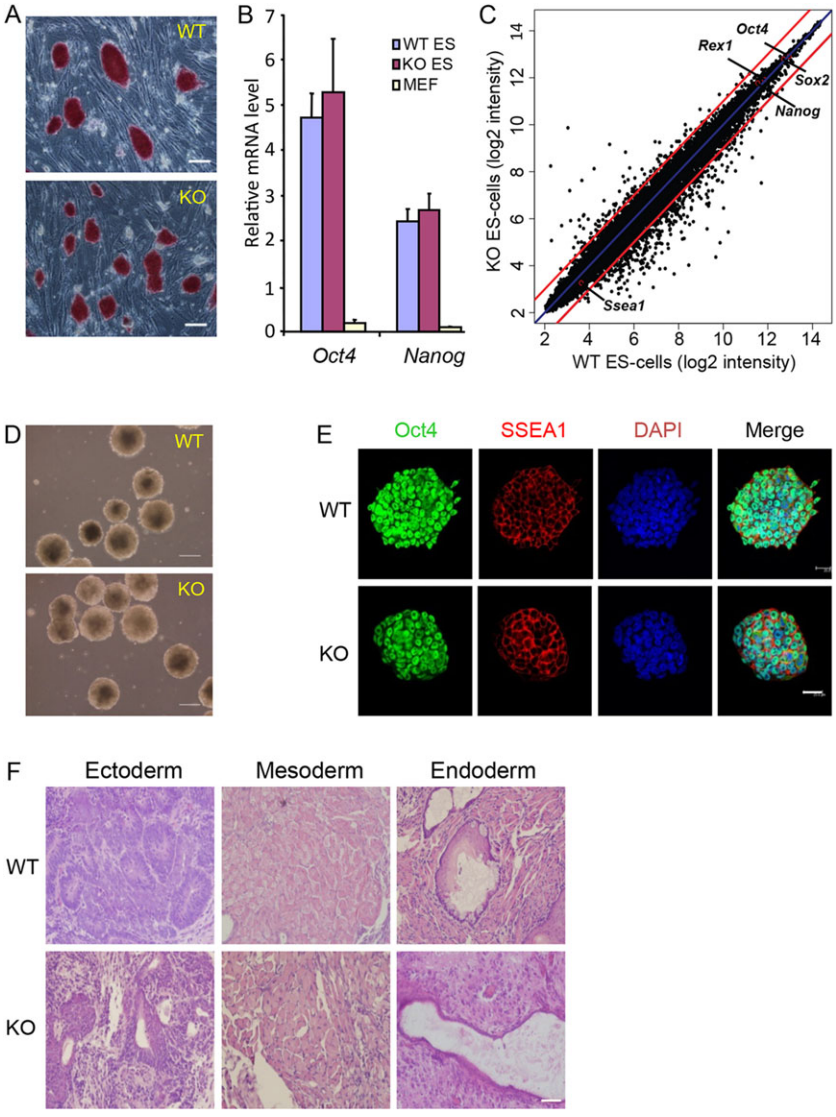

Fig. 1. Characterization of *Med23* KO ESCs. (A) Wild-type (WT) and KO ESCs were plated at clonal density with feeder cells for 2 days and then stained for alkaline phosphatase activity (red). Scale bars: 100 µm. (B) The expression of *Oct4* and *Nanog* was measured by qRT-PCR and normalized to the *EF2* mRNA expression levels. (C) Scatter plots comparing global gene expression patterns between wild-type and KO ESCs; red lines indicate the linear equivalent and twofold changes in gene expression levels between the samples. (D) Morphology of embryoid bodies (EBs) from wild-type and KO ESCs at day 4 of spontaneous differentiation culture. Scale bars: 200 µm. (E) Immunostaining for OCT4 and SSEA1 in EBs derived from wild-type and KO ESCs. Scale bar: 25 µm. (F) Various tissue types were present in teratomas derived from *Med23* KO ESCs, including ectoderm (neuroepithelium), mesoderm (muscle) and endoderm (ciliated epithelium). Scale bar: 100 µm.

Development (2015) 142, 465-476 doi:10.1242/dev.112946

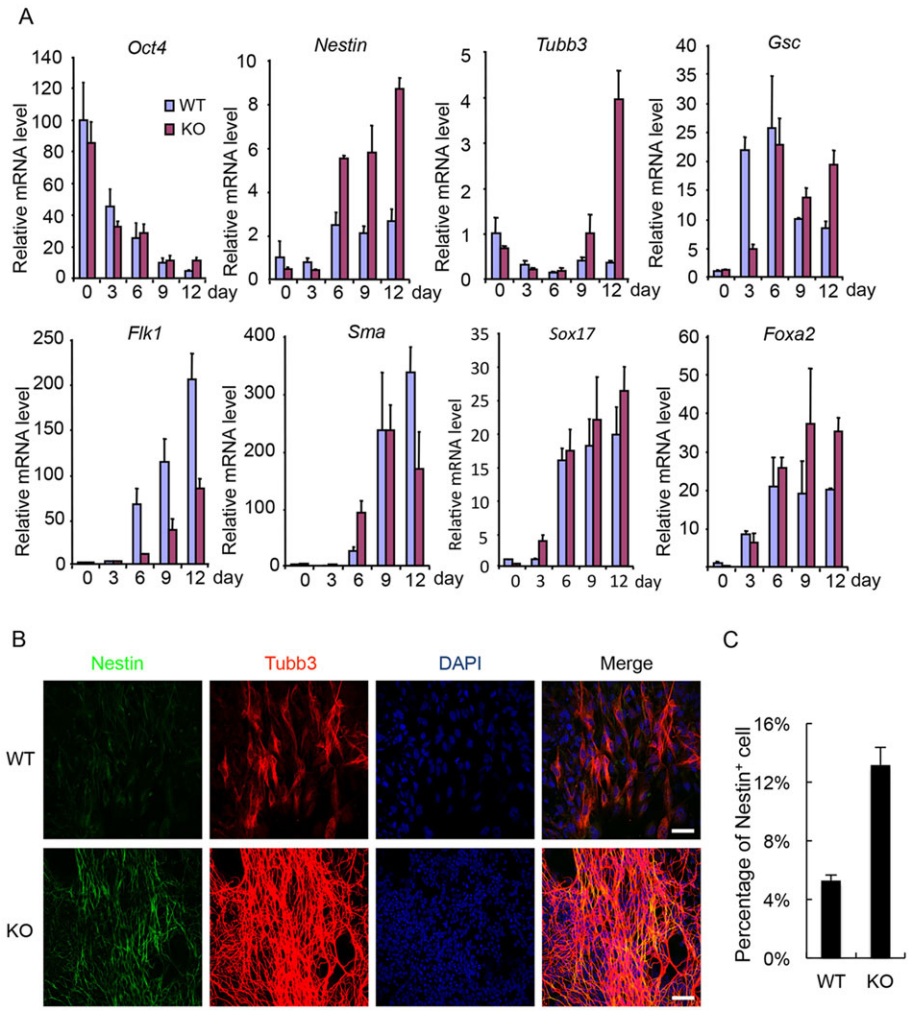

Fig. 2. Enhanced neuroectoderm specification in spontaneous differentiation of *Med23* KO ESCs. (A) Expression levels of genes indicative of self-renewal (*Oct4* and *Nanog*), ectoderm (*Nes* and *Tubb3*), mesoderm (*Gsc*, *Flk1* and *Sma*) and endoderm (*Sox17* and *Foxa2*) were determined by qRT-PCR under ESC culture conditions and spontaneous differentiation culture conditions for 3, 6, 9 and 12 days. Expression levels were normalized to the *Gapdh* mRNA expression level. (B) Wild-type and KO ESCs were induced to form cells of all three germ layers by spontaneous differentiation for 9 days, and were then immunostained for NES (green), TUBB3 (red) and DAPI (blue). Scale bars: 50 µm. (C) Percentage of NES+ cells; wild-type and KO ESCs were induced to spontaneous differentiation, and anti-NES immunostaining was combined with FACS analysis at day 12.

(Fig. 2A). Compared with wild-type cells, the expression of the ectoderm-specific gene nestin (*Nes*) was more upregulated from day 6 to day 12, and *β-tubulin* III (*Tubb3*) was more upregulated at day 12 of spontaneous differentiation in KO cells. By contrast, there seemed to be no consistent, significant difference in the expression levels of the mesoderm-specific genes *Gsc* and *Sma* (*Ighmbp2* – Mouse Genome Informatics) and of the endoderm marker genes *Sox17* and *Foxa2* between the differentiating KO and wild-type cells (Fig. 2A).

Similar results were obtained when immunostaining for the markers of neural progenitors (NES) and immature neurons (TUBB3), which both were significantly enhanced in KO cells at day 9 under differentiation condition (Fig. 2B). To quantitate the difference of wild-type and KO cell differentiation, immunostaining for NES combined with FACS analysis revealed that the percentage of NES+ cells was 13.16% in KO at day 12, compared with 5.27% in WT (Fig. 2C). Therefore, our observations suggest that loss of MED23 renders the ESCs prone toward the neural lineage, and that MED23 plays a specific, restrictive role in mESCs along the neural pathway.

Med23 deficiency enhances neural differentiation of ESCs in both adherent monolayer and suspension cultures

To verify the role of MED23 in neuroectoderm differentiation, we induced neural differentiation of wild-type and KO ESCs, using the serum-free adherent monoculture method (Ying et al., 2003). Wild-type and KO ESCs grown in N2B27 medium were harvested at days 1, 2, 3, 4 and 7. Consistent with our observations of the spontaneously differentiating cells, the expression levels of multiple neural lineage genes, such as *Blbp* (*Fabp7* – Mouse Genome Informatics), *Pou3f3*, *Cp*, *Fgfrs* and *Nes*, were strikingly upregulated at days 4 and 7 in *Med23* KO cells compared with wild-type cells (Fig. 3A). Moreover, immunofluorescence staining with antibodies against the neural markers NES, MAP2 (Fig. 3B) and BLBP (supplementary material Fig. S1D) revealed that the expression levels of these proteins were greatly enhanced in KO cells compared with wild-type cells.

To test whether the function of MED23 in neural differentiation is independent of the N2B27 medium and the monolayer culture, we performed an additional neural differentiation assay using the serum-free EB formation (SFEB) method (Watanabe et al., 2005). In the SFEB culture, both wild-type and KO ESCs were able to aggregate and form EBs. Gene expression levels in EBs were monitored using real-time PCR after 0, 2, 4, 6 and 8 days of SFEB culture. Consistent with monolayer differentiation, the expression levels of the ESC marker genes *Oct4* (*Pou5f1* – Mouse Genome Informatics) and *Nanog* decreased more rapidly in *Med23* KO EBs than in wild-type EBs. However, expression of neural cell markers, such as *Sox1*, *Blbp*, *Pou3f3*, *Cp*, *Nes* and *Tubb3*, increased significantly faster and to higher levels in *Med23* KO EBs (supplementary material Fig. S2A), thus suggesting more efficient and rapid differentiation in *Med23* KO EBs. Differentiating EBs

Development (2015) 142, 465-476 doi:10.1242/dev.112946

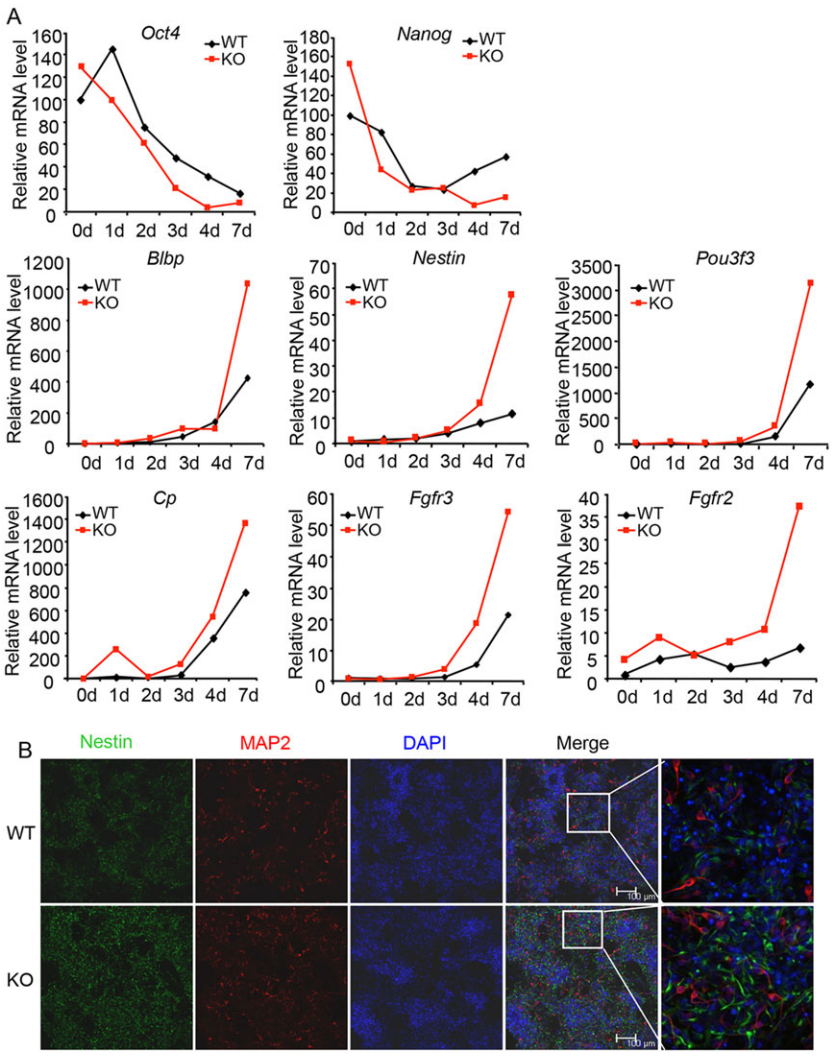

Fig. 3. *Med23* deletion promotes neural differentiation in N2B27 culture. (A) ESCs were cultured under monolayer differentiation conditions in the presence of N2B27. Expression levels of marker genes for ESC self-renewal and neural precursor cells were measured by qRT-PCR. *Gapdh* mRNA expression was used for normalization. (B) Immunostaining for NES (marker of neural progenitors) and MAP2 (marker of mature neurons) in wild-type and KO cells at day 7 of monolayer culture. Scale bars: 100 µm.

derived from wild-type and KO ESCs were harvested at day 6, sectioned and stained with antibodies specific against OCT4, SOX2, BLBP and NES. Co-immunostaining of OCT4and SOX2 exhibited distinct expression patterns in the differentiating wild-type and KO EBs. OCT4+SOX2+ cells and OCT4−SOX2+ cells, indicating ESCs and neural precursor cells, respectively, were counted in multiple sections from multiple EBs. OCT4−SOX2+ cells represented 46.1% of the cells in KO EBs, compared with 7.3% of the cells in WT (supplementary material Fig. S2B,C), indicating a ∼6.5-fold increase in the number of neural precursor cells derived from the *Med23*-depleted cells. However, the numbers of OCT4+SOX2+ cells (ESCs) were less than onefold lower in KO EBs than in wild-type EBs. Moreover, co-immunofluorescent staining for BLBP and NES was enhanced by 35% and 48%, respectively, in KO EBs compared with wild-type EBs, as quantified by fluorescence intensity (data not shown). Thus, two independent methods of cell differentiation, using distinct culture conditions, demonstrate that depletion of *Med23* promotes rapid and efficient neural differentiation of mouse ESCs.

To further verify the role of MED23 in neural differentiation, mouse *Med23* was reintroduced into the KO cells using retroviral transduction. Exogenous expression of mouse MED23 in stable cell lines was examined by western blot (Fig. 4A). Only one line of cells showed the re-expression of MED23, and this line was used for further analysis. After cells were induced to differentiate, RT-PCR confirmed the greatly enhanced expression of neural markers in KO cells (Fig. 4B). Significantly, exogenous expression of mouse MED23 partially rescued the enhanced neural differentiation in KO cells, as assessed by the expression of *Sox1*, *Nes*, *Blbp* and *Pou3f3* and by immunostaining for NES and BLBP (Fig. 4B,C). Collectively, these results, coupled with the experiments in both adherent monolayer and suspension cultures, demonstrate that MED23 is crucial for regulating neural differentiation of ESCs.

Two other Mediator components, MED1 and MED15, do not alter neural differentiation

Med23 depletion does not impair the integrity of the Mediator complex, as demonstrated in our earlier study (Wang et al., 2009). To ascertain the specificity of MED23 in neural differentiation among the Mediator subunits, we probed the functions of two other subunits, MED1 and MED15, during ESC differentiation.

A previous study showed that Mediator *Med1* is required for PPARG2-mediated adipogenesis (Ge et al., 2002); however, whether it is required for neural specification is not yet known. We established stable cell lines by viral-mediated knockdown of *Med1* and *Med23* in R1 ESCs. Consistently, we observed that knocking down *Med23* leads to enhanced neural differentiation. However, interference with the expression of another Mediator component, *Med1*, failed to change the speed and efficiency of neural differentiation (supplementary material Fig. S3).

Development (2015) 142, 465-476 doi:10.1242/dev.112946

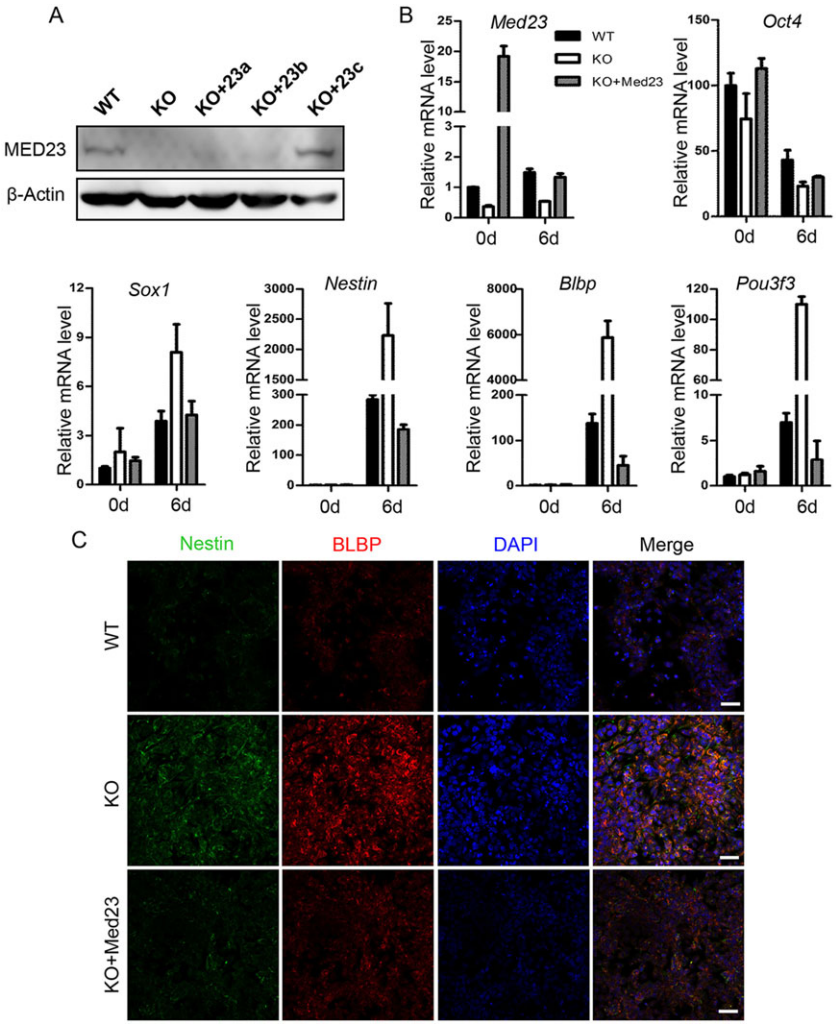

Fig. 4. Enhanced neural differentiation is reversed by re-expression of *Med23*. (A) Immunoblot of MED23 in wild-type, *Med23* KO and *Med23* KO+exogenous *Med23* ESCs. (B) Expression of marker genes for ESC self-renewal and neural precursors were measured by qRT-PCR. *Gapdh* mRNA was used as internal control. (C) Immunostaining for NES and BLBP in differentiated cells derived from wild-type, *Med23* KO and *Med23* KO +exogenous *Med23* ESCs, respectively. Scale bars: 50 µm.

A previous study found that MED15 contributes to mesoendoderm specification in *Xenopus* (Kato et al., 2002), but it remains to be determined whether MED15 controls the early cell fates of ESCs. In this study, we observed that viral-mediated knockdown of *Med15* did not affect the features of the ESCs (supplementary material Fig. S4A,B); however, consistent with the study in *Xenopus*, MED15 is specifically required for endoderm differentiation in mouse ESCs (supplementary material Fig. S4C). The specificity was shown by the fact that *Med15* depletion resulted in reduction in endoderm markers, such as FOXA2, AFP and SOX17 (supplementary material Fig. S4C), but failed to affect neural differentiation (supplementary material Fig. S4D). These observations further emphasized the specific role of MED23 in neural lineage. Collectively, these results suggest that different Mediator subunits contribute to the distinct cell lineage regulation during early development.

MED23 regulates neural specification by modulating BMP4 signaling

Multiple signaling pathways have been shown to impact the neural induction from ESCs, such as BMP, FGF and WNT signaling at the gastrulation stage (Baker et al., 1999; Wilson et al., 2000; Stern, 2005). In this context, we examined whether MED23 affects these signal pathways. A transcriptome analysis was performed to compare the gene expression patterns between *Med23* KO and wild-type ESCs under the standard ESC culture condition, which represents the starting point of ESC differentiation. Only very few genes from the WNT signaling pathway (the core β-catenin pathway and WNT/sFRP families) and the FGF/MAPK pathway [except *Egr1*, a prototype MED23-target gene (Wang et al., 2005)] that displayed strong defects as a result of the *Med23* KO (Fig. 5A, columns 1, 2, 4 and 5). However, we observed the downregulation of multiple BMP/SMAD pathway member genes, such as *Id1*, *Id2*, *Bmp4*, *Bmpr1a*, *Dusp9* and *Coch* (Fig. 5A, column 3) that have been described as BMP-target genes by previous studies (Li et al., 2012). In contrast to the significantly altered gene expression of the BMP4/SMAD pathway, the subunit genes of the TFIID complexes were only moderately changed by *Med23* deletion (Fig. 5A, column 5), thereby suggesting that *Med23* deficiency might specifically attenuate BMP4 signaling. As a genome-wide analysis also revealed that *Bmp4* expression levels were largely reduced in KO ESCs, we examined the expression of BMP4-target gene *Id1* and *Id2* by qRT-PCR and found that expression of both genes was reduced (Fig. 5B). Importantly, qRT-PCR also verified that the expression of *Bmp4* was greatly reduced in *Med23* KO ESCs during the entire neural differentiation process in adherent monolayer culture (Fig. 5B). In addition, the level of phospho-Smad1/5/8, representing BMP signaling activity, was significantly reduced in both normal culture and serum starvation condition in KO ESCs compared with wild-type ESCs, suggesting that BMP signaling is reduced in KO ESCs (Fig. 5C). Therefore, *Med23* deficiency impairs *Bmp4* expression, which might be the crucial event that results in the downregulation of the entire pathway.

Development (2015) 142, 465-476 doi:10.1242/dev.112946

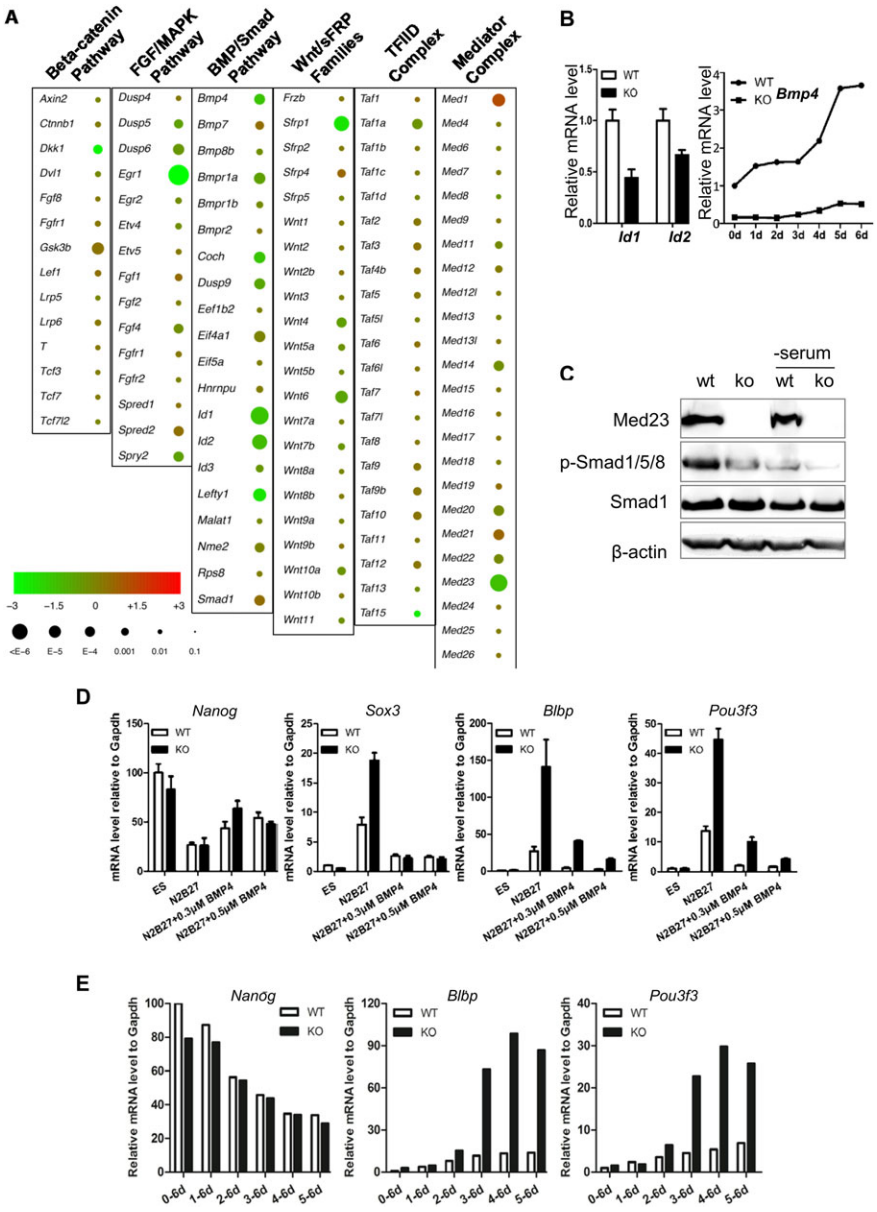

Fig. 5. *Med23* deletion attenuates BMP4 signal. (A) Difference in expression (log2 [KO/WT]) and statistical significance between *Med23*-depleted and wild-type ESCs. (B) qRT-PCR measured the expression of *Id1* and *Id2* in ESCs, and the expression of *Bmp4* in ESCs and during differentiation in adherent monolayer culture. (C) Identification of phospho-Smad1/5/8 under ESC or serum starvation culture conditions. (D) Expression of pluripotency markers and neural markers was examined by qRT-PCR at day 6 of monolayer differentiation; the expression was normalized to *Gapdh* mRNA levels. (E) Cells cultured by N2B27, with recombinant hBMP4 added at different time points; pluripotency markers and neural markers were examined by qRT-PCR.

BMP signaling has been previously shown to repress neural differentiation in mouse ESCs (Tropepe et al., 2001; Ying et al., 2003). Given that MED23 impacts neural differentiation through BMP4, addition of BMP4 should be able to repress the enhanced neural differentiation in the *Med23* KO ESCs culture. Indeed, we observed that, whereas *Med23* deficiency promoted ESC neural differentiation, addition of BMP4 significantly abrogated the enhanced neural differentiation (Fig. 5D). Consequently, neural differentiation became equivalent between wild-type and KO ESCs at day 6 of differentiation. To further define the time window during which BMP4 functions during neural differentiation, recombinant BMP4 was added to the N2B27 monolayer culture at different time points of the wild-type and KO ESC differentiation. We defined the day on which the ESCs were seeded as differentiation day 0 and examined the neural marker at day 6. We found that the most significant inhibition of neural differentiation was achieved when BMP4 was added during day 1-3, whereas the addition of BMP4 at other time points failed to change the course of differentiation (Fig. 5E). This suggests that ESCs are most sensitive to BMP4-mediated block of neural differentiation at the early phase of differentiation.

MED23 regulates *Bmp4* expression through controlling the activity of the ETS family member ETS1

To understand the molecular mechanism by which *Med23* deficiency inhibits *Bmp4* expression, we first performed a promoter analysis for the *Bmp4* gene. Sequence analysis of the *Bmp4* promoter region revealed the presence of multiple putative binding sites for the transcription factor ETS1, an ETS family member. The putative ETS1-binding sites (EBS) could be separated as distal region 'A' and proximal region 'B', respectively (Fig. 6A). The transcription factor ETS family members are defined by a conserved DNA-binding domain and a common consensus target sequence, GGA(A/T) (Hollenhorst et al., 2011). Our previous study shows that the ETS family member ELK1 interacts with MED23 (Wang et al., 2009), we thus tested whether ETS1 could cooperate with MED23 to control the expression of *Bmp4*.

Development (2015) 142, 465-476 doi:10.1242/dev.112946

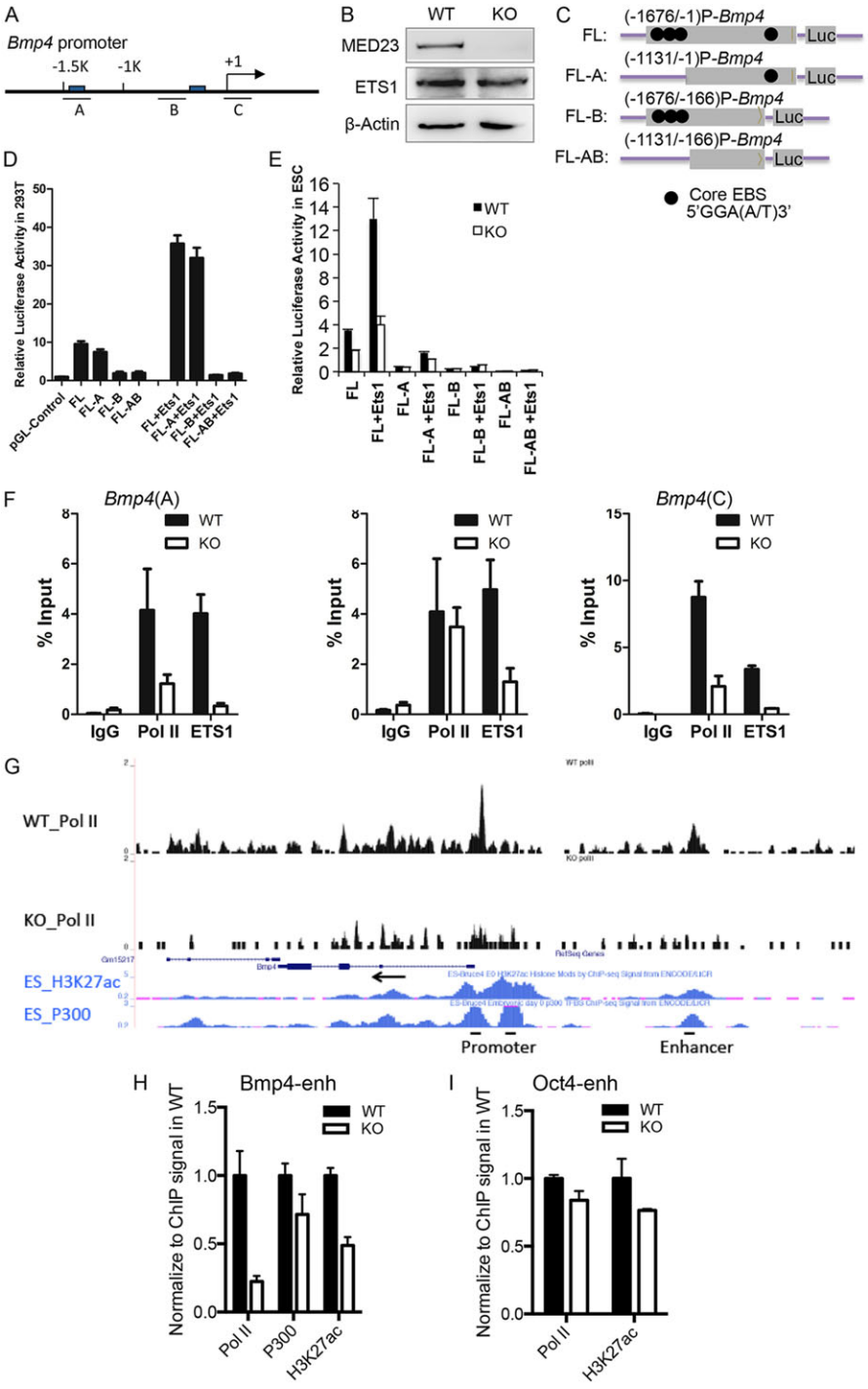

Fig. 6. MED23 affects *Bmp4* expression via ETS1. (A) EBS (ETS-binding site) and primer-binding sites on *Bmp4* promoter region. (B) Examination of ETS1 protein levels between KO and WT by western blot. (C) Reporter plasmids were constructed as full length (FL), and vectors with deletion of three distal ETS1-binding sites (FL-A), deletion of two proximal ETS1-binding sites (FL-B) and deletion of both distal and proximal ETS1-binding sites (FL-AB). (D,E) 293T cells and ESCs were transfected with reporter plasmids with or without the ETS1 expression vector, and the activity was determined (relative to *Renilla* activity). pGL-basic vector was used as a control (pGL-Control). (F) ChIP experiments were performed using antibodies against ETS1 and Pol II, and IgG as control. The precipitated DNA was analyzed by RT-PCR, with primers targeting the *Bmp4* promoter region (A,B) and coding region (C). The primer sequences are provided in supplementary material Table S1. The relative binding level of each factor was calculated by normalization to the input DNA. (G) ChIP-seq analysis of Pol II enrichment at *Bmp4* locus in wild-type and KO ESCs. Compared with H3K27ac and p300 ChIP-seq data of ENCODE, an enhancer region of *Bmp4* was predicted as shown. (H,I) *MED23* depletion impaired *Bmp4* enhancer activity indicated by ChIP assays of Pol II, P300 and H3K27ac, but did not change the *Oct4* enhancer activity.

We first determined whether ETS1 regulates *Bmp4* expression. The promoter region of murine *Bmp4* was subcloned into a reporter vector with or without the deletions of the region 'A' and/or 'B'. The following cloned luciferase constructs were used: the full-length (FL) promoter sequence from −1 to −1676 bp; FL with region 'A' deleted (FL-A), from −1 to −1311 bp; FL with region 'B' deleted, from −166 to −1676 bp; and FL with both region 'A' and 'B' deleted, from −166 to −1311 bp (Fig. 6C). The luciferase activity driven by FL, FL-A, FL-B and FL-AB was evaluated in co-transfection experiments in 293T cells. As control, pGL-Control was transfected with empty pGL3. The luciferase activity of the promoters FL-B and FL-AB was reduced by 80% compared with the FL promoter, whereas the reduction of luciferase activity of FL-A was only 21% (Fig. 6D), suggesting that region 'B' is more important than 'A' for the ETS1 activity. In addition, overexpression of ETS1 enhanced the luciferase activity of promoter FL and FL-A more than threefold, but the luciferase activity of FL-B and FL-AB could not be induced by ETS1 (Fig. 6D), thus again suggesting that the ETS1-binding site 'B' is crucial for ETS1 in activating *Bmp4* promoter. Consistent with these results in 293T cells, we also observed that the luciferase activity of FL was lower in KO ESCs compared with WT, and that exogenous expression of ETS1 enhanced the luciferase activity of the promoter FL threefold in wild-type ESCs, but only onefold in KO ESCs (Fig. 6E). Furthermore, deletion of either 'A' or 'B' impaired

Development (2015) 142, 465-476 doi:10.1242/dev.112946

promoter activity significantly (Fig. 6E), suggesting that the *Bmp4* promoter regions 'A' and 'B' are both required for ETS1-driven *Bmp4* promoter activity in ESCs.

We next examined whether both endogenous ETS1 and MED23 are required for *Bmp4* transcription. Chromatin immunoprecipitation (ChIP) assays were performed to measure the binding of ETS1 and POL II (POLR2F – Mouse Genome Informatics) at the *Bmp4* locus when cells were cultured under the serum-free condition that closely mimics the neural differentiation condition. We found that both ETS1 and Pol II constitutively bind to the *Bmp4* promoter at both regions 'A' and 'B'. However, ETS1 binding at both regions 'A' and 'B' of the *Bmp4* promoter was greatly reduced in KO cells (Fig. 6F), despite the fact that the expression level of ETS1 protein seemed to be equal in both wild-type and KO ESCs (Fig. 6B).

We were intrigued by the observation that Pol II binding reduced significantly at distal promoter region 'A' (Fig. 6F), suggesting that ETS1 probably also regulates *Bmp4* transcription through an enhancer. Previous studies indicated that the Mediator complex cooperates with the cohesin complex to contribute to chromatin architecture (Kagey et al., 2010), and collaborates with diverse transcription factors to establish a 'super enhancer' for cell fate determination (Whyte et al., 2013). This information prompted us to examine whether an enhancer might be involved in the *Bmp4* gene regulation. Predicted by the ChIP-seq data of H3K27ac and P300 from ENCODE, a putative enhancer region −10 kb upstream of the *Bmp4* transcription start site was identified (Fig. 6G). We then tested whether the Mediator subunit MED23 regulates this enhancer function of the *Bmp4* gene. When comparing Pol II ChIP-seq signals on *Bmp4* between wild-type and KO ESCs, we found that enrichment of Pol II was decreased in KO ESCs at both the promoter and the putative enhancer regions of *Bmp4*, suggesting that MED23 depletion might have disrupted the interplay between the promoter and enhancer regions of *Bmp4* (Fig. 6G). To verify the effect of MED23 depletion on the enhancer activity, we performed ChIP assays to examine the possible changes of three typical enhancer markers: Pol II, P300 and H3K27ac at the Bmp4 putative enhancer region in the KO ESCs. The results showed that MED23 deficiency reduced their enrichments at the *Bmp4* enhancer, suggesting that MED23 can alter promoter-enhancer loop confirmation on *Bmp4* for its transcriptional control (Fig. 6H). By contrast, the enrichment of Pol II and H3K27ac at the *Oct4* enhancer region was largely unchanged in either wild-type or KO cells (Fig. 6I), which is consistent with the fact that the *Oct4* expression is independent of MED23 (Fig. 1B,C). Taken together, these data suggest that the presence of MED23 favors the ETS1 binding to facilitate promoter-enhancer communication on *Bmp4*, which might account for the higher *Bmp4* expression in wild-type ESCs. We are currently unable to co-IP the endogenous ETS1 and MED23, probably due to the transient and dynamic nature of ETS1:MED23 interaction. However, based on the experimental evidence shown above, we propose that MED23 might functionally associate with ETS1, directly or indirectly, to mediate the enhancer-promoter interaction, thus controlling *Bmp4* expression (Fig. 7F).

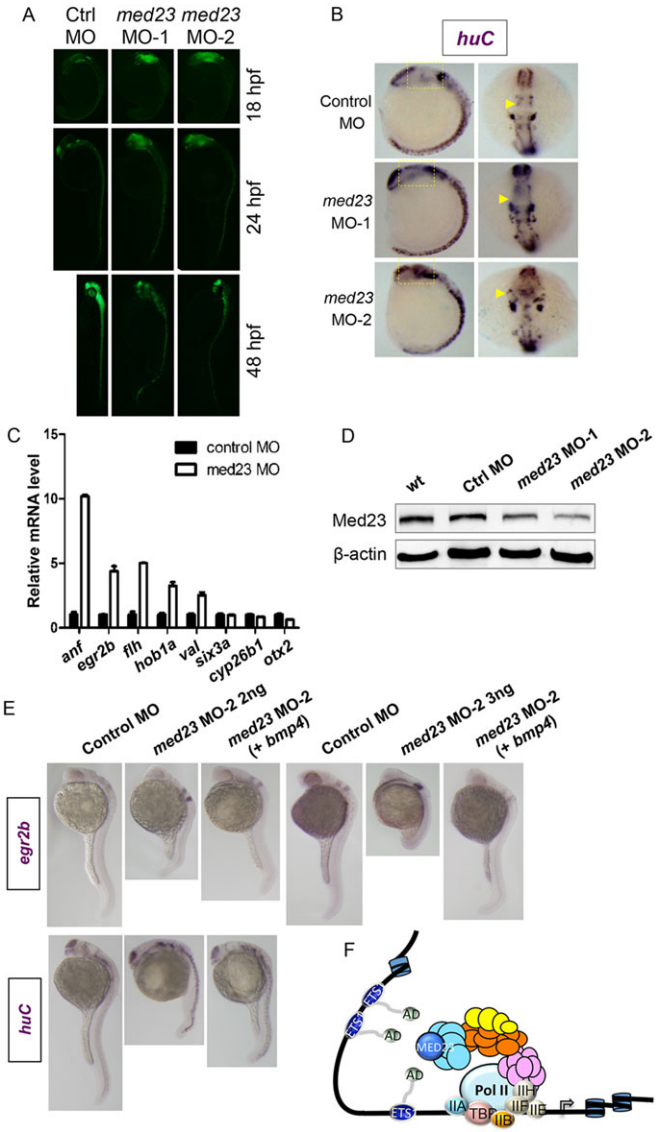

Fig. 7. ME23 regulates neural development via *bmp4* in zebrafish. (A) GFP signals of control MO-treated or *med23* MO-treated *HuC*-GFP transgenic zebrafish during development process. (B) *In situ* hybridization of *huC* mRNA levels in control MO zebrafish and *med23* morphants at 15 hpf; the mid-hindbrain is indicated by frame or arrow. (C) Marker gene expression of telencephlon (*anf*), diencephalon (*flh*), hindbrain (*egr2b*, *hoxb1a*, *cyp26b1*), forebrain and midbrain (*six3a*, *otx2*) at 24 hpf; the expression is normalized to *Rbl13a* mRNA levels. (D) Protein levels for Med23 in WT, control MO zebrafish and *med23* morphants at 24 hpf; β-actin was used as an internal control. (E) *In situ* hybridization of *huC* and *egr2b* mRNA levels in control MO zebrafish and *med23* morphants at 24 hpf. (F) Model for ETS1-driven *Bmp4* transcription modulated by MED23.

Knockdown of *med23* in zebrafish results in enhanced neural development that is reversible with *bmp4* mRNA co-injection

During the early development of zebrafish *med23* is ubiquitously expressed (supplementary material Fig. S5A). Our recent study showed that *med23* MO-injected embryos (morphants) showed abnormal phenotypes and precocious development of vascular smooth muscle (Yin et al., 2012). As *Med23* KO mESCs are prone to neural differentiation, we repeated the *med23* MO-injection experiment in zebrafish to explore the role of *med23* in neural development. In this study, two antisense morpholino oligonucleotides (MO-1 and MO-2) were used to inhibit the expression of *med23* in zebrafish as shown by western blot (Fig. 7D). We observed that *med23* morphants generally had a survival time of 5-7 days post fertilization (supplementary material Fig. S5E) and an apophysis phenotype in the dorsal brain (supplementary material Fig. S5B). To determine whether Med23 regulates neural development *in vivo*, we monitored the early neural development in *huC-gfp* transgenic zebrafish, using the *huC* expression to indicate the pan-neural development. We found that

Development (2015) 142, 465-476 doi:10.1242/dev.112946

HuC-GFP signals can be detected as early as 12 h post fertilization (hpf) in *med23* morphants, but not in the control MO embryos (12 hpf). Consistently, the total mRNA levels of endogenous *huC* and *egr2b* were also increased in both morphants compared with the control at 6 hpf and 9 hpf (supplementary material Fig. S5C), which was further verified by *in situ* hybridization for *huC* at 12 hpf (supplementary material Fig. S5D). Moreover, we observed that *HuC*-driven GFP expression was greatly enhanced in morphant brains at 18 hpf and 24 hpf compared with the control group (Fig. 7A). The enhanced GFP expression seems to localize mainly at a particular hindbrain region, as indicated by *in situ* hybridization for *huC* at 15 hpf (Fig. 7B) and for *huC* and *egr2b* at 24 hpf (Fig. 7E). Accordingly, the expression levels of endogenous *anf* (telencephlon), *flh* (diencephalon), *egr2b* and *hoxb1a* (hindbrain) were upregulated in morphants at 24 hpf compared with the control group, although some neural markers, such as *cyp26b1* (hindbrain), *six3a* (forebrain) and *otx2* (midbrain) were not changed after *med23* knockdown (Fig. 7C). Notably, we also observed that the *HuC*-GFP signal became weaker in *med23* morphants at 48 hpf compared with the control group, probably as result of precocious neuronal differentiation (Fig. 7A).

Previous studies have shown that BMP activity affects dorsoventral (DV) patterning at all anteroposterior (AP) levels of the neural plate and is required for patterning neurons at all DV levels of the central nervous system (CNS) (Barth et al., 1999), and Bmp signaling might regulate the acquisition of a DV and AP identity of a cell simultaneously (Tucker et al., 2008). In our zebrafish study, we observed that the DV axes of *med23* morphants shortened and the AP axes elongated compared with the control group (Fig. 7E). Given that *Med23* regulates BMP/SMAD signaling in mESCs, we are interested in whether the enhanced neural development in *med23* morphants is also regulated by a Bmp4 signal. *In situ* hybridization revealed that the increased expression of *huC* in the brain and spinal cord of *med23* morphants could be repressed after co-injection of low level *bmp4* mRNA (3 pg/per embryo) to a level comparable to that of control MO zebrafish embryos (Fig. 7E). Interestingly, zebrafish embryos injected with a higher concentration of *med23* MO presented a more severe phenotype; this phenotype was reversed (or rescued) when embryos were co-injected with *bmp4* mRNA (Fig. 7E). This experiment suggests that Bmp4 is a crucial effector in Med23-modulated early neural development of zebrafish. Overall, the zebrafish data seem to be consistent with our observations on the role of MED23 in mESC differentiation, reinforcing the notion that MED23 impacts on early neural development via BMP4 signaling.

DISCUSSION

Previous studies demonstrated that all Mediator complex subunits are generally expressed at high levels in ESCs compared with differentiated fibroblasts, and Mediator contributes to the communication between the enhancer and proximal promoter regions of the pluripotency genes in ESCs (Kagey et al., 2010). This suggests that Mediator participates in the regulation of ESC function. *Med23*-depleted ESCs were shown to maintain the integrity of the Mediator complex, as evaluated through co-IP and gel filtration assays (Stevens et al., 2002; Wang et al., 2009). To understand the role of MED23 in regulating stem cell identity, we performed numerous assays, including gene profiling, pluripotency marker analysis, EB formation and teratoma formation, and we demonstrated that loss of *Med23* did not alter the self-renewal and pluripotency of ESCs. As both wild-type and KO ESCs maintain the stem cell properties, we analyzed whether wild-type and KO ESCs might have different differentiation potentials, using an unbiased spontaneous EB differentiation assay. Interestingly, *Med23* deficiency specifically promoted neural differentiation in an unbiased differentiation assay. Two distinct neural differentiation assays, N2B27 monolayer and KSR suspension culture, further verified this observation.

Neural specification from ESCs is regulated by multiple signals, such as WNT signaling, BMP/SMAD and FGF/MAPK pathway. By gene profiling, we detected that BMP/SMAD signaling was attenuated and *Bmp4* expression was reduced in *Med23* KO ESCs. An in-depth mechanistic study revealed that MED23 regulates ETS1-driven *Bmp4* expression. Importantly, enhanced neural differentiation was attenuated when BMP4 was added back to the KO ESC culture, or when the *med23* MO was co-injected with *bmp4* mRNA, suggesting that BMP4 is indeed an effector in MED23-regulated neural development. To further understand how exactly MED23 controls ETS1-driven *Bmp4* expression, we employed ChIP and ChIP-seq assays. We showed that MED23 depletion might disrupt the connection between ETS1 and the transcription machinery, and compromise the promoter-enhancer interaction of *Bmp4*, thus resulting in the decreased *Bmp4* expression and enhanced neural differentiation. *Bmp4* is a well-known neural lineage blocker gene, although its own regulation during development is not well studied. Our work describes for the first time that how *Bmp4* is regulated by MED23 during neural differentiation of ESCs. This expands our understanding of the function of the Mediator complex in long-distance gene regulation, and provides a novel mechanistic basis of how different Mediator subunits determine different cell lineages (Yin and Wang, 2014).

Besides the BMP pathway, multiple signaling pathways are involved in regulating neural differentiation from ESCs. Previous studies suggested that FGF/MAPK signaling is required for neural fate determination (Kunath et al., 2007; Stavridis et al., 2007; LaVaute et al., 2009) and that MED23 is a target of this pathway (Wang et al., 2005). We therefore also examined the activity of the MAPK pathway in *Med23* KO ESCs during differentiation. Phospho-ERK1/2 levels, representing FGF/MAPK pathway activity, were analyzed by western blot and seemed to be similar in KO and wild-type ESCs. However, ERK1/2-phosphorylation showed a slight increase in KO cells at early differentiation (day 1), which is consistent with a previous study showing that FGF-induced MAPK/ERK activity is required for neural lineage commitment of ESCs (Kunath et al., 2007) (supplementary material Fig. S6A). In addition to FGF/MAPK, WNT signaling also extensively affects neuroectodermal differentiation from ESCs (Aubert et al., 2002; Sato et al., 2004; Lindsley et al., 2006). In our study, we observed that phospho-β-catenin was increased and total β-catenin was reduced in KO ESCs and in KO ESC-derived cells during differentiation (day 1-2) compared with WT, suggesting that the WNT signaling activity was probably attenuated (supplementary material Fig. S6A). Paradoxically, we found that the expression of the WNT target genes *Axin2* and *Sox3* were increased in KO cells compared with wild-type cells during differentiation (supplementary material Fig. S6B). Despite these observations, only a few genes from the WNT signaling pathway, as examined by gene profiling, displayed obvious defects (Fig. 5A, column 4), thus suggesting that WNT signaling activity was not changed as a result of *Med23* depletion. Overall, our data showed that MED23 might regulate neural differentiation mainly through modulating BMP signaling.

Growing evidence supports the notion that the Mediator subunits control diverse development processes with subunit specificity (Kato et al., 2002; Wang et al., 2006; Yang et al., 2006; Lin et al., 2007; Chen

Development (2015) 142, 465-476 doi:10.1242/dev.112946

et al., 2010). Our previous studies demonstrated that *Med23* deficiency reduced adipocyte differentiation and increased SMC differentiation (Wang et al., 2009; Yin et al., 2012), suggesting the important roles of MED23 in mesoderm development. In this study, however, in multiple ESC differentiation assays, we did not observe any dramatic and consistent changes for mesoderm markers, such as *Sma* and *Flk1*, which might be due to the ESC differentiation representing an early stage of development. In contrast to the mild changes of *Flk1* and *Sma*, the expression of both *Nes* and *Tubb3* was greatly increased in KO ESCs in multiple differentiation assays. Therefore, we focused on the role of MED23 in neural differentiation using the ESC differentiation system. In this study, enhanced neural differentiation by *Med23* depletion was observed in two independent ESC lines and under three distinct culture conditions, including spontaneous EB differentiation, N2B27 monolayer and KSR suspension culture. However, knockdown of two other Mediator components, *Med1* or *Med15*, did not change the neural differentiation potentials (supplementary material Figs S3 and S4), and *Med15* knockdown specifically blocked the endoderm differentiation (supplementary material Fig. S4). Using zebrafish to study the role of *Med23* on neural development *in vivo*, we observed that *med23* knockdown facilitated neural development ahead of schedule compared with control embryos, and led to precocious neuronal differentiation. Taken together, these data demonstrate that, despite the Mediator subunit MED23 having pleiotropic effects on multiple cell fate determination at different development stages, MED23 does play a specific role at an early stage of neural development.

Thus, targeting Mediator MED23 might provide a rapid and efficient method to generate a large amount of neural progenitor cells from ESCs or induced pluripotent stem cells (iPSCs), which might lead to new therapeutic strategies for neurodegenerative diseases.

MATERIALS AND METHODS

Animals

Wild-type zebrafish (*Danio rerio*) and HuC transgenic zebrafish were obtained and maintained in the National Zebrafish Resources of China (Shanghai, China). All zebrafish were maintained with an automatic fish-housing system (ESEN, China) at 28°C. Embryos and larvae were raised on a 14-10 h light-dark cycle in 10% Hank's solution.

The nude mice were obtained from Shanghai Laboratory Animal Center, Chinese Academy of Sciences. All animal handling procedures were approved by the Institutional Animal Care and Use Committee of Shanghai Institutes for Biological Sciences.

ESC culture

All ESCs were maintained in knockout Dulbecco's modified Eagle's medium (DMEM) (Invitrogen) supplemented with 15% fetal bovine serum (Hyclone), 1× nonessential amino acids (Gibco), 1% L-glutamine (Gibco), 1% penicillin/streptomycin (Gibco), 1×10^3 units/ml LIF (ESGRO, Chemicon) and 0.1 mM β-mercaptoethanol (β-ME; Sigma). Cells were grown in a humidified incubator at 37°C and 5% CO_2, routinely passaged at 75% confluency and were fed daily. LW murine ESCs, 129-derived (a kind gift from Dr Hong Wu, UCLA, USA), were maintained on 0.2% gelatin-coated plates. R1 murine ESCs were maintained on a feeder cell layer of irradiated mouse embryonic fibroblasts.

Spontaneous differentiation

Undifferentiated ESCs were cultivated as EBs in hanging drops for 2 days, followed by culturing in suspension for an additional 3 days. The EBs were then were plated onto gelatin-coated tissue culture plates. For immunostaining assays, cells were cultured in gelatin-coated 4-well chamber slides. Cells were cultured in ES medium lacking LIF, and the medium was changed every other day.

Neural differentiation methods

The method used for monoculture differentiation has been described previously (Pollard et al., 2006). Undifferentiated ESCs were dissociated and plated onto 0.2% gelatin-coated plates at a density of $0.8\text{-}1.2\times10^4/cm^2$ in N2B27 medium. After the first 2 days, medium was renewed daily. N2B27 is a 1:1 mixture of DMEM/F12 (Gibco) supplemented with modified N2 [25 μg/ml insulin, 100 μg/ml human transferrin, 6 ng/ml progesterone, 16 μg/ml putrescine, 30 nM sodium selenite and 50 μg/ml bovine serum albumin fraction V (Gibco)] and neurobasal medium (Gibco) supplemented with B27 (Gibco). For immunostaining, cells were transferred to 4-well chamber slides pre-treated with poly-L-ornithine (50 μg/ml) and laminin A (10 μg/ml). For SFEB culture, differentiation medium was prepared as follows: G-MEM supplemented with 5% knockout serum replacement (KSR) (Invitrogen), 2 mM glutamine, 1 mM pyruvate, 0.1 mM nonessential amino acids and 0.1 mM β-ME. Briefly, 5×10^4 cells per 1 ml differentiation medium were seeded into 6-cm bacterial dishes (5 ml). ESCs spontaneously aggregated to form EBs in serum-free suspension cultures within 1 day. Medium was changed every two days. RNA was extracted from differentiating EBs on days 2, 4, 6 and 8 for gene expression assays. EBs were fixed and sectioned for immunofluorescent staining on day 6.The day on which ESCs were seeded to differentiate was defined as day 0.

Immunofluorescence

Cells were washed with PBS twice, fixed in 4% paraformaldehyde and incubated for 1 h in blocking buffer (PBS, 2% BSA and 0.2% Triton X-100). Primary antibodies were diluted in blocking buffer and applied overnight at 4°C. After three washes in PBS, secondary antibodies diluted in blocking buffer were applied for 1 h at room temperature. After three washes by PBS, nuclei were stained with DAPI (1:1000) for 4 min. Antibodies used for immunostaining were as follows: anti-NES (Santa Cruz, sc-21249; 1:50); anti-BLBP (Abcam, ab32423; 1:200); anti-OCT4 (Santa Cruz, sc-8628; 1:100); anti-SOX2 (Abcam, ab59776; 1:200); anti-MAP2 (Chemicon, MAB5622; 1:200) and anti-SSEA1 (Santa Cruz, sc-21702; 1:100).

Real-time PCR and western blotting

Methods for real-time PCR and western blot were described previously (Wang et al., 2009). Total RNA was isolated from cells using TRIzol (Invitrogen). The first-strand cDNA was generated using MMLV transcriptase (Promega), and real-time PCR was performed in triplicate using a SYBR Green PCR master mix in an Eppendorf Mastercycler. All values were normalized to the level of *EF2* or *Gapdh* mRNA, which is constitutively expressed and not changed during the time course of the experiments. Primer sequences used in the experiments are included in the supplementary material Table S1. The western blot was performed using an ECL kit (Pierce) based on the manufacturer's recommendations. HRP-conjugated secondary antibodies were purchased from Jackson Laboratory.

Teratoma formation

After nude mice were anesthetized with diethyl ether, 1.5×10^6 ESCs were injected subcutaneously into the dorsal flank. Tumors were surgically dissected from the mice 26 days after injection. Samples were fixed in 4% paraformaldehyde and embedded in paraffin. Sections were stained with hematoxylin and eosin.

Retroviral constructs and infection

Establishing stable cell lines to knock down a gene of interest was based on the manufacturer's recommendation (Clontech). For knockdown of *Med23*, *Med15* and *Med1* in ESCs, retrovirus-mediated siRNA expression was used. The targeted sequence was determined using the Whitehead Institute siRNA designing tool. As recommended by Clontech for the RNAi-Ready pSIREN-RetroQ system, two complementary oligos for each targeted sequence were designed, annealed and ligated into the *Bam*HI/*Eco*RI-linearized pSIREN-RetroQ vector. The resulting construct, upon packaging into retroviruses, allows for the stable expression of the siRNA hairpin

Development (2015) 142, 465-476 doi:10.1242/dev.112946

specific for the target gene. The sequences of the oligonucleotides are provided in supplementary material Table S1. Generation of retroviruses has been described previously (Wang et al., 2009).

Morpholino, mRNA synthesis and microinjection

Morpholino antisense oligonucleotides (MO) were obtained from Gene Tools, and the sequence information of morpholinos is provided in supplementary material Table S1. To generate mRNAs, full-length *bmp4* (zebrafish) genes were subcloned into a pCDNA3 vector (cloning primer sequences are listed in supplementary material Table S1) and synthesized using the mMessage mMachine kit (Ambion). For all microinjection experiments, a volume of 1 nl was injected into one- to two-cell stage embryos. Zebrafish maintenance and breeding were carried out as previously described (Westerfield, 1993). Embryos were raised at 28.5°C and staged as previously described (Kimmel et al., 1995).

Whole-mount *in situ* hybridization

RNA antisense probes were synthesized using a DIG RNA labeling kit (Roche, 11175025910). Zebrafish embryos of the appropriate stages were collected and dechorionated when needed. The embryos were fixed in PBS containing 4% PFA and dehydrated in methanol at −20°C. Whole-mount *in situ* hybridization (WISH) was performed as described previously (Yue et al., 2009) with some modifications. Hybridization signals were detected by the addition of an anti-DIG antibody conjugated with alkaline phosphatase (Roche, 11093274910) and the enzyme substrates BCIP/NBT (Vector Labs, SK5400).

Microarray analysis

Mouse genome-wide gene expression analysis was performed using Affymetrix Mouse Gene 430 2.0 array. Six arrays were probed with cDNA synthesized from total RNA isolated from wild-type and *Med23* knockout ESCs. Data are deposited at GEO under accession number GSE64500.

ChIP, ChIP-seq and data analysis

ChIP assays were performed as described previously (Wang et al., 2005), and immunoprecipitated DNA was quantified by real-time PCR. The following antibodies were used: anti-ETS1 (Santa Cruz, sc-350X; 1:100); anti-Pol II (Santa Cruz, sc-899; 1:100); anti-P300 (Santa Cruz, sc-585; 1:100); anti-H3K4me1 (Abcam, ab8895; 1:500) and anti-H3K27ac (Abcam, ab4729; 1:500). The primers for analyzing the ChIP DNA are provided in supplementary material Table S1. ChIPed DNA was prepared for ChIP-seq and data analysis as described previously (Huang et al., 2012).

Acknowledgements

We thank Dr Arnie Berk (UCLA, Los Angeles, USA) for reagents and Dr Jiulin Du (Institute of Neuroscience, Shanghai, China) for help with the zebrafish experiments.

Competing interests

The authors declare no competing or financial interests.

Author contributions

G.W. and W.Z. conceived and designed the experiments and wrote the manuscript. W.Z. performed most experiments. X.Y. and Y.L. provided experimental support and assisted in data analysis. D.L., L.S., N.J. and J.L. provided reagents and suggestions.

Funding

This work was supported in part by grants from the Chinese Academy of Sciences (CAS) [XDA01010401], the National Natural Science Foundation of China (NSFC) [31271452 and 81030047] and the Chinese Ministry of Science and Technology (MOST) [2011CB510104 and 2014CB964702]. G.W. is a scholar of the 'Hundred Talent Program' of the Chinese Academy of Science.

Supplementary material

Supplementary material available online at
http://dev.biologists.org/lookup/suppl/doi:10.1242/dev.112946/-/DC1

References

Aubert, J., Dunstan, H., Chambers, I. and Smith, A. (2002). Functional gene screening in embryonic stem cells implicates Wnt antagonism in neural differentiation. *Nat. Biotechnol.* **20**, 1240-1245.

Baker, J. C., Beddington, R. S. P. and Harland, R. M. (1999). Wnt signaling in Xenopus embryos inhibits bmp4 expression and activates neural development. *Genes Dev.* **13**, 3149-3159.

Balamotis, M. A., Pennella, M. A., Stevens, J. L., Wasylyk, B., Belmont, A. S. and Berk, A. J. (2009). Complexity in transcription control at the activation domain-mediator interface. *Sci. Signal.* **2**, ra20.

Barth, K. A., Kishimoto, Y., Rohr, K. B., Seydler, C., Schulte-Merker, S. and Wilson, S. W. (1999). Bmp activity establishes a gradient of positional information throughout the entire neural plate. *Development* **126**, 4977-4987.

Chen, W., Zhang, X., Birsoy, K. and Roeder, R. G. (2010). A muscle-specific knockout implicates nuclear receptor coactivator MED1 in the regulation of glucose and energy metabolism. *Proc. Natl. Acad. Sci. USA* **107**, 10196-10201.

Crook, J. M. and Kobayashi, N. R. (2008). Human stem cells for modeling neurological disorders: accelerating the drug discovery pipeline. *J. Cell. Biochem.* **105**, 1361-1366.

Ge, K., Guermah, M., Yuan, C.-X., Ito, M., Wallberg, A. E., Spiegelman, B. M. and Roeder, R. G. (2002). Transcription coactivator TRAP220 is required for PPAR gamma 2-stimulated adipogenesis. *Nature* **417**, 563-567.

Hollenhorst, P. C., McIntosh, L. P. and Graves, B. J. (2011). Genomic and biochemical insights into the specificity of ETS transcription factors. *Annu. Rev. Biochem.* **80**, 437-471.

Huang, Y., Li, W., Yao, X., Lin, Q.-J., Yin, J.-W., Liang, Y., Heiner, M., Tian, B., Hui, J. and Wang, G. (2012). Mediator complex regulates alternative mRNA processing via the MED23 subunit. *Mol. Cell* **45**, 459-469.

Kagey, M. H., Newman, J. J., Bilodeau, S., Zhan, Y., Orlando, D. A., van Berkum, N. L., Ebmeier, C. C., Goossens, J., Rahl, P. B., Levine, S. S. et al. (2010). Mediator and cohesin connect gene expression and chromatin architecture. *Nature* **467**, 430-435.

Kato, Y., Habas, R., Katsuyama, Y., Näär, A. M. and He, X. (2002). A component of the ARC/Mediator complex required for TGF beta/Nodal signalling. *Nature* **418**, 641-646.

Kimmel, C. B., Ballard, W. W., Kimmel, S. R., Ullmann, B. and Schilling, T. F. (1995). Stages of embryonic development of the zebrafish. *Dev. Dyn.* **203**, 253-310.

Kirouac, D. C. and Zandstra, P. W. (2008). The systematic production of cells for cell therapies. *Cell Stem Cell* **3**, 369-381.

Kunath, T., Saba-El-Leil, M. K., Almousailleakh, M., Wray, J., Meloche, S. and Smith, A. (2007). FGF stimulation of the Erk1/2 signalling cascade triggers transition of pluripotent embryonic stem cells from self-renewal to lineage commitment. *Development* **134**, 2895-2902.

LaVaute, T. M., Yoo, Y. D., Pankratz, M. T., Weick, J. P., Gerstner, J. R. and Zhang, S.-C. (2009). Regulation of neural specification from human embryonic stem cells by BMP and FGF. *Stem Cells* **27**, 1741-1749.

Li, Z., Fei, T., Zhang, J., Zhu, G., Wang, L., Lu, D., Chi, X., Teng, Y., Hou, N., Yang, X. et al. (2012). BMP4 Signaling Acts via dual-specificity phosphatase 9 to control ERK activity in mouse embryonic stem cells. *Cell Stem Cell* **10**, 171-182.

Lin, X., Rinaldo, L., Fazly, A. F. and Xu, X. (2007). Depletion of Med10 enhances Wnt and suppresses Nodal signaling during zebrafish embryogenesis. *Dev. Biol.* **303**, 536-548.

Lindsley, R. C., Gill, J. G., Kyba, M., Murphy, T. L. and Murphy, K. M. (2006). Canonical Wnt signaling is required for development of embryonic stem cell-derived mesoderm. *Development* **133**, 3787-3796.

Malik, S. and Roeder, R. G. (2010). The metazoan Mediator co-activator complex as an integrative hub for transcriptional regulation. *Nat. Rev. Genet.* **11**, 761-772.

Muñoz-Sanjuán, I. and Brivanlou, A. H. (2002). Neural induction, the default model and embryonic stem cells. *Nat. Rev. Neurosci.* **3**, 271-280.

Pollard, S. M., Benchoua, A. and Lowell, S. (2006). Neural stem cells, neurons, and glia. *Methods Enzymol.* **418**, 151-169.

Sato, N., Meijer, L., Skaltsounis, L., Greengard, P. and Brivanlou, A. H. (2004). Maintenance of pluripotency in human and mouse embryonic stem cells through activation of Wnt signaling by a pharmacological GSK-3-specific inhibitor. *Nat. Med.* **10**, 55-63.

Singh, N. and Han, M. (1995). sur-2, a novel gene, functions late in the let-60 ras-mediated signaling pathway during Caenorhabditis elegans vulval induction. *Genes Dev.* **9**, 2251-2265.

Stavridis, M. P., Lunn, J. S., Collins, B. J. and Storey, K. G. (2007). A discrete period of FGF-induced Erk1/2 signalling is required for vertebrate neural specification. *Development* **134**, 2889-2894.

Stern, C. D. (2005). Neural induction: old problem, new findings, yet more questions. *Development* **132**, 2007-2021.

Stevens, J. L., Cantin, G. T., Wang, G., Shevchenko, A., Shevchenko, A. and Berk, A. J. (2002). Transcription control by E1A and MAP kinase pathway via Sur2 mediator subunit. *Science* **296**, 755-758.

Tropepe, V., Hitoshi, S., Sirard, C., Mak, T. W., Rossant, J. and van der Kooy, D. (2001). Direct neural fate specification from embryonic stem cells: a primitive

Development (2015) 142, 465-476 doi:10.1242/dev.112946

mammalian neural stem cell stage acquired through a default mechanism. *Neuron* **30**, 65-78.

Tucker, J. A., Mintzer, K. A. and Mullins, M. C. (2008). The BMP signaling gradient patterns dorsoventral tissues in a temporally progressive manner along the anteroposterior axis. *Dev. Cell* **14**, 108-119.

Wang, G., Balamotis, M. A., Stevens, J. L., Yamaguchi, Y., Handa, H. and Berk, A. J. (2005). Mediator requirement for both recruitment and postrecruitment steps in transcription initiation. *Mol. Cell* **17**, 683-694.

Wang, X., Yang, N., Uno, E., Roeder, R. G. and Guo, S. (2006). A subunit of the mediator complex regulates vertebrate neuronal development. *Proc. Natl. Acad. Sci. USA* **103**, 17284-17289.

Wang, W., Huang, L., Huang, Y., Yin, J.-W., Berk, A. J., Friedman, J. M. and Wang, G. (2009). Mediator MED23 links insulin signaling to the adipogenesis transcription cascade. *Dev. Cell* **16**, 764-771.

Watanabe, K., Kamiya, D., Nishiyama, A., Katayama, T., Nozaki, S., Kawasaki, H., Watanabe, Y., Mizuseki, K. and Sasai, Y. (2005). Directed differentiation of telencephalic precursors from embryonic stem cells. *Nat. Neurosci.* **8**, 288-296.

Westerfield, M. (1993). *The Zebrafish Book: A Guide for the Laboratory Use of Zebrafish (Brachydanio rerio)*. Eugene, OR: University of Oregon Press.

Whyte, W. A., Orlando, D. A., Hnisz, D., Abraham, B. J., Lin, C. Y., Kagey, M. H., Rahl, P. B., Lee, T. I. and Young, R. A. (2013). Master transcription factors and mediator establish super-enhancers at key cell identity genes. *Cell* **153**, 307-319.

Wilson, S. I., Graziano, E., Harland, R., Jessell, T. M. and Edlund, T. (2000). An early requirement for FGF signalling in the acquisition of neural cell fate in the chick embryo. *Curr. Biol.* **10**, 421-429.

Yang, F., Vought, B. W., Satterlee, J. S., Walker, A. K., Jim Sun, Z.-Y., Watts, J. L., DeBeaumont, R., Saito, R. M., Hyberts, S. G., Yang, S. et al. (2006). An ARC/Mediator subunit required for SREBP control of cholesterol and lipid homeostasis. *Nature* **442**, 700-704.

Yin, J.-W. and Wang, G. (2014). The Mediator complex: a master coordinator of transcription and cell lineage development. *Development* **141**, 977-987.

Yin, J.-W., Liang, Y., Park, J. Y., Chen, D., Yao, X., Xiao, Q., Liu, Z., Jiang, B., Fu, Y., Bao, M. et al. (2012). Mediator MED23 plays opposing roles in directing smooth muscle cell and adipocyte differentiation. *Genes Dev.* **26**, 2192-2205.

Ying, Q.-L., Stavridis, M., Griffiths, D., Li, M. and Smith, A. (2003). Conversion of embryonic stem cells into neuroectodermal precursors in adherent monoculture. *Nat. Biotechnol.* **21**, 183-186.

Yue, R., Kang, J., Zhao, C., Hu, W., Tang, Y., Liu, X. and Pei, G. (2009). Beta-arrestin1 regulates zebrafish hematopoiesis through binding to YY1 and relieving polycomb group repression. *Cell* **139**, 535-546.